

Lasers in Manufacturing Conference 2019

# Effect of gas flow on spatter formation in deep penetration welding at high welding speeds

Leander Schmidt<sup>a\*</sup>, Klaus Schrickler<sup>a</sup>, Jean Pierre Bergmann<sup>a</sup>, Steen Hickethier<sup>a</sup>

<sup>a</sup>Technische Universität Ilmenau, Production Technology Group, Gustav-Kirchhoff-Platz 2, 98693 Ilmenau, Germany

---

## Abstract

Spatter formation is a major issue in deep penetration welding with solid state lasers at high welding speeds from 8 up to 20 m/min. To avoid spatter formation, the use of local adjustable shielding gas flows was investigated. By using a precisely adjustable shielding gas supply, the effect of argon was characterized by welding stainless steel (1.4301/X5CrNi18-10/ AISI304). Different flow rates and spatial orientations were examined. The influence of the gas flow on the keyhole formation and the resulting spatter formation was recorded by means of HV-camera and subsequently analyzed by image processing (number, velocity and trajectory of spatters, shape of the keyhole aperture). A reduction of spatters up to 91 % at welding speeds up to 16 m/min was reached. Finally, a description of the general mechanisms between gas flow, keyhole fluctuations, pressure conditions and melt pool dynamics is given.

Keywords: welding; macro processing; spatter formation; low-spatter welding; influence of shielding gas

---

## 1. Introduction

Laser beam welding of stainless steels is highly important for several applications, for example in welding of pipes. Due to new developments in solid-state lasers towards higher power classes, the process has a high potential for increasing economic efficiency by increasing welding speeds. However, the welding speed cannot be increased at now, because process instabilities occur. At welding speeds above 8 m/min, the stability of the keyhole becomes even more important than in the low speed regime. Based on the speed-dependent piercing process, the keyhole tilts against the feed direction, which leads to a higher energy absorption at the keyhole front (Weberpals, 2010). Following, a metal vapor flow is initiated, which is

---

\* Corresponding author. Tel.: +49-3677-693854; fax: +49-3677-691660  
E-mail address: leander.schmidt@tu-ilmenau.de

directed towards the keyhole rear wall. By the interaction of the vapor flow and the molten material, an impulse is transmitted to the melt pool. This results in the formation of melt pool fluctuations and can lead to the detachment of molten material (Zhang et al., 2013; Volpp, 2017). For the extraction of one single spatter, the kinetic energy of the fluid element in the melt must be greater than the sum of the kinetic energy of the droplet and the surface energy of the melt (Hügel et al., 2009). Thereby, spatter formation is decisively dependent on welding speed and laser intensity (Fabbro et al., 2007). In this context, it is well known that the thermo- and fluid dynamic changes at welding speeds of 8–20 m/min results in an increasing keyhole instability and a high loss of mass (Nagel et. al, 2019; Schmidt et. al, 2018). Thereby, the stability of the keyhole is described by a pressure balance of opening and closing pressures (equation 1, according to Beck, 1996).

$$p_{abl} + p_v - p_0 = p_\sigma + p_h + p_{dyn} \quad (1)$$

The physical quantities are  $p_{abl}$  as recoil pressure,  $p_v$  as vapor pressure,  $p_0$  as atmospheric pressure,  $p_\sigma$  as surface tension pressure,  $p_h$  as hydrostatic pressure, and  $p_{dyn}$  as hydrodynamic pressure.

In order to reduce spatter formation, numerous variants have been examined for manipulating the pressure balance. Thereby, the use of local shielding gas flows represents a particularly attractive solution. Kamikuki et al., 2002 characterized the influence of a lateral shielding gas flow at a welding speed of 1 m/min. Using the gas flow, a decreasing number of pores and a reduced spatter formation could be determined. Furthermore, it was possible to detect an enlargement of the keyhole aperture, which was mentioned as the reason for the spatter reduction (changed outflow conditions of the metal vapor flow). In a further investigation, Fabbro, 2010 obtained comparable results up to a welding speed of 5 m/min. The influence of the flow orientation (leading and trailing positioning) could be demonstrated, whereby no significant difference could be found. In contrast, Herrmann, 2006 was able to determine a more positive effect of a trailing flow orientation. This was attributed to a reduced interaction of the gas flow with the outflowing metal vapor. Further, Zhang et al., 2011 was able to simulate the influence of the gas flow. Depending on the flow rate, an enlargement of the keyhole could be obtained. It could be established, that the pressure increase inside the keyhole contributes to a stabilization of the keyhole wall and thus ensures a constant flow cross-section of the escaping metal vapor flow. Consequently, the impulse transfer from the vapor flow to the melt is reduced and less spatters occurs.

However, the investigations have been carried out up to a welding speed of 5 m/min. A study about the influence of a local gas flow at the welding speeds above 5 m/min has not been sufficiently investigated so far. Therefore, this publication examines the influence of a local shielding gas flows on spatter formation during deep penetration welding of high-alloy steel (1.4301, X5CrNi18-10, AISI304) at welding speeds of 8 to 16 m/min. For this purpose, a novel experimental setup was developed in order to describe the effect of flow rate, angle of incidence and flow orientation (leading and trailing).

## 2. Experimental setup

The investigations were carried out for deep penetration welding of stainless austenitic steel 1.4301 (X5CrNi18-10, AISI 304) with a constant welding depth of  $\approx 1.7 \text{ mm} \pm 0.1 \text{ mm}$ . For this purpose, a disk laser (TruDisk 5000.75, Trumpf Laser und Systemtechnik GmbH, Germany) with a stationary welding optic (Fig. 1 a) was used. The laser is characterized by a wavelength of 1030 nm, a fiber diameter of 200  $\mu\text{m}$  and a spot diameter of 274  $\mu\text{m}$  at a maximum power of 5 kW. The samples (150 mm x 40 mm x 2mm) were handled and clamped at the front of a six-axis robot (KR 60HA, Kuka AG, Germany). The process was recorded by means of a Photron SA-X2 high-speed camera, which was equipped with a Navitar zoom lens. Using a narrow-band

filter with a center wavelength of 808 nm, it was possible to record the process on the basis of thermal radiation. Further, the captured data were analyzed using a Matlab-based image analysis. So, it was possible to determine the trajectories of spatter formation (superposition of sequential frames) as well as the angle of detachment and the particle speed. The loss of mass was determined by a high-precision balance (PLU 2000-3A, Kern und Sohn GmbH, Germany). The weight was measured before and after the welding process, based on a weld seam length of 150 mm. Furthermore, the experimental setup was equipped with a newly developed shielding gas nozzle unit (Fig. 2 b). The unit could be positioned using linear guides with an accuracy of 0.05 mm and a reproducibility of 0.02 mm. Besides the variation of the angle of incidence ( $\phi = 20^\circ - 48^\circ$ ), the nozzle orientation (leading/trailing) was changed. Moreover, the unit was equipped with a coaxial alignment laser, which allowed the marking of the interaction area between the gas flow and the specimen. The nozzle tube of the unit had an inner diameter of 1.2 mm and were positioned in a constant distance from the nozzle tip to the specimen surface of 5 mm. All experiments were carried out using argon and repeated for three times.

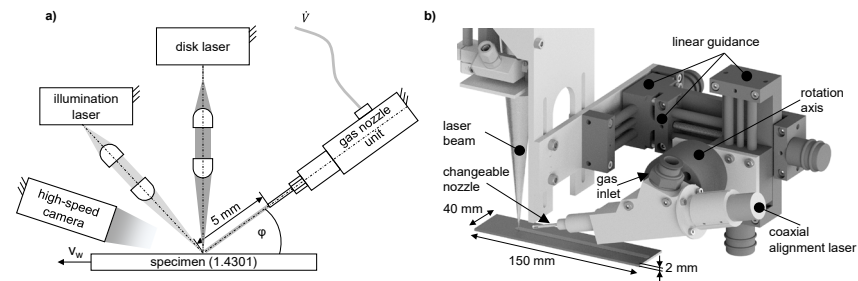


Fig. 1. (a) Schematic experimental setup; (b) shielding gas nozzle unit

### 3. Results and discussion

#### 3.1. Influence of the angle of incidence and the flow rate at trailing flow orientation

In the first step, the influence of the angle of incidence was examined in the case of a trailing shielding gas configuration during a variation of the welding speed ( $v_w = 8 - 16$  m/min, see Fig. 2).

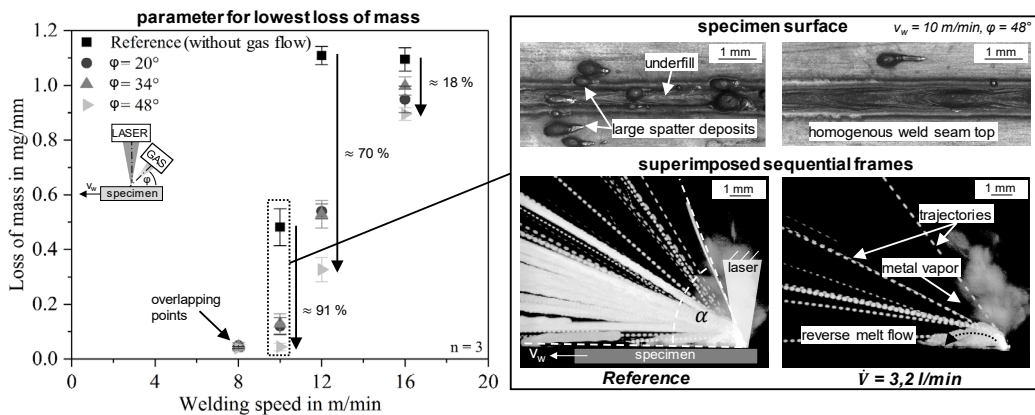


Fig. 2. Loss of mass as a function of welding speed at varying angles of incidence

Based on the reference process without shielding gas supply, there was a significant increase in the loss of mass above welding speeds of 10 m/min. The maximum of 1.1 mg/mm was determined at a welding speed of 12 m/min. A further increase of welding speed to 16 m/min showed no significant effect on the resulting loss of mass. Using the local shielding gas flow, the loss of mass could be notably reduced by up to 91 % at 10 m/min and by up to 70 % at 12 m/min. Consequently, the number of spatters adhering to the specimen surface was considerably decreased as well as the formation of weld seam underfill could be avoided. Therefore, a homogenous weld seam top was observed. By varying the flow rate from 1.6 l/min up to 6.4 l/min, it was not possible to see a significant influence on the loss of mass, on the spatter trajectories and respectively on the angles of detachment. However, at flow rates of more than 6.4 l/min, the formation of humps could be observed (see Schmidt et al., 2019). Another effect could be determined by varying the angle of incidence. Thus, rising angles of incidence, especially at a welding speed of 12 m/min, resulted in the highest reduction of the loss of mass. Further, an increased welding depth ( $\approx 6\%$ ) could be achieved, which can be attributed to a higher energy absorption inside the keyhole due to the less fluctuating keyhole.

By comparing the high-speed recordings, it was possible to see a significant effect by the gas flow (Fig. 3). In this way, the filamentary spatter detachment of the keyhole rear wall of the reference process could be prevented by the use of the gas. The melt pool swelling at the keyhole rear wall was noticeably less fluctuating as well as a significant extended melt pool length could be determined. Based on the reduced keyhole fluctuations, the formation of a reverse flow from the keyhole rear wall into the downstream melt pool could be seen. Further, a decreasing keyhole length could be measured (up to 20 %). Consequently, the keyhole aperture becomes more circular than elliptical using the gas flow. By comparing the longitudinal sections, it was not possible to detect any different effect. However, the cross sections indicate, that the use of the gas flow resulted in a near-surface widening of the weld seam top (up to 19 %). In contrast to the gas-assisted process, an underfill could be observed at the weld seam top of the reference process, which is based on the high loss of mass.

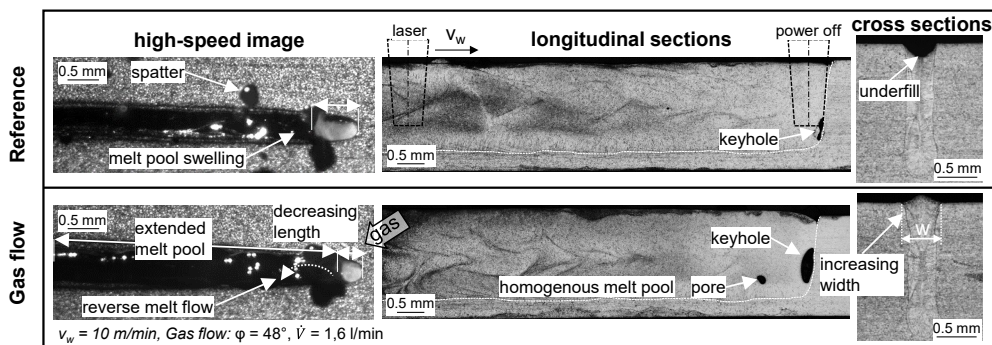


Fig. 3. Melt pool dynamic and cross/longitudinal sections for reference and gas assisted process by a welding speed of 10 m/min

The reduction of the loss of mass, which was achieved by the local shielding gas flow, can be attributed to a general mechanism. Following, the internal keyhole pressure is increased by the additional applied gas pressure  $p_{\text{gas}}$  (equation 1). As a result, the forces for opening the keyhole predominate the forces for closing the keyhole. Thus, the keyhole is stabilized and fluctuates less. This allows the metal vapor to escape more uniformly, so that the interaction of the vapor flow and the melt is reduced and a smaller amount of spatters occur. Furthermore, due to the increased keyhole stability, a higher amount of energy can be absorbed inside the keyhole. In the experiment, this effect could be observed by a widening of the seam top as well as by a minimally increased welding depth. According to the law of continuity ( $Q = v \cdot \rho \cdot A = \text{const.}$ ), the weld

seam widening results in an increase of the flow area. Thus, the flow velocity of the keyhole surrounding melt is lowered and the formation of melt pool swellings is reduced. Consequently, the keyhole fluctuates less and thus the process is stabilized.

### 3.2. Influence of a leading flow orientation

In the next step, the influence of a leading flow orientation was investigated. For this purpose, the process parameters of the lowest loss of mass of the trailing flow orientation ( $\phi = 48^\circ$ ,  $\dot{V} = 1.6 - 6.4$  l/min) were applied in the experiment.

First, the influence of the flow rate was investigated (Fig. 4 a). It was shown, that the spatter detachment (spatter trajectories) were significantly affected by flow rates of 3.2 l/min and above. Based on a spatter detachment against welding direction at a flow rate of 1.6 l/min, the spatter trajectories changed into a spatter detachment in welding direction ( $\geq 3.2$  l/min). As a result, the keyhole became instable and spatter formation was increased. Consequently, the flow rate was set to 1.6 l/min for further investigations.

In the following step, the effect of the leading flow orientation was compared to the trailing flow orientation by measuring the resulting loss of mass (Fig. 4 b). By using the leading orientation, it was possible to achieve comparable reductions in the loss of mass at welding speeds of 8 – 16 m/min as reached before in a trailing flow orientation. However, in interpreting the results, it is necessary to make a differentiation in relation to the welding speed.

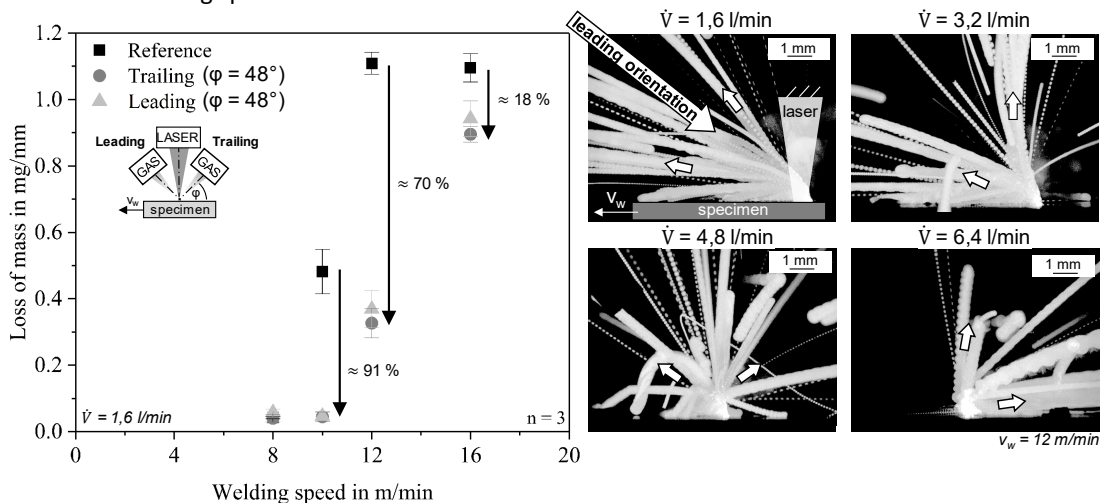


Fig. 4. (a) Effect of flow rate at leading flow orientation; (b) comparison of loss of mass between a leading and trailing flow orientation

- At a welding speed of 10 m/min, the leading flow orientation had a positive effect on the formation and stability of the keyhole (see also Fig. 5). Thus, a reduced keyhole fluctuation and a less spatter formation could be observed. As previously seen with a trailing flow orientation, it was possible to determine a formation of a reverse melt flow into the downstream melt pool. Further, an extended melt pool length as well as a reduced keyhole length could be measured. The increased stability of the keyhole resulted in a significantly reduced number of spatters adhering to the specimen surface. Therefore, it can be said that the effect of a trailing as well as a leading flow orientation is comparable for a welding speed of 10 m/min up to a flow rate of 1.6 l/min.

- At a welding speed of 12 m/min, the use of the leading flow orientation led to a deterioration of the welding process. In this case, the high reduction of the loss of mass is deceptive. Despite the effect of the formation of a reduced keyhole length as well as a wider weld seam top, the rear side of the keyhole was not sufficiently stabilized. Following, ongoing fluctuations of the keyhole led to a further melt ejection. However, the ejected spatter had a lower kinetic energy than in the reference process. As a result, a large percentage of the spatter hit the upper side of the melt pool again. Thereby the formation of a weld seam underfill was prevented. In contrast, the other part resulted in an increase in spatter adhesion on the specimen surface. Consequently, the surface quality of component was reduced. In conclusion it can be said, that the use of a trailing flow orientation is preferable to a leading flow orientation at a welding speed of 12 m/min.

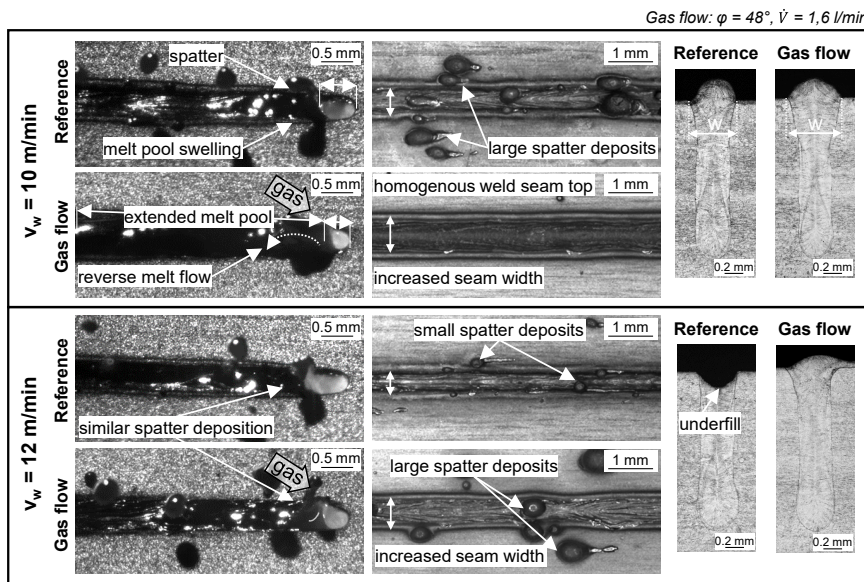


Fig. 5. Influence of a leading flow orientation of the melt pool dynamics and weld seam quality for a welding speed of 10 and 12 m/min

The negative effect of a leading flow orientation can be explained by a general mechanism. At welding speeds above 8 m/min, the increase in the flow velocities inside the melt pool leads to the formation of a melt pool swelling at the keyhole rear wall (Fabbro et al., 2007). If this area cannot be stabilized, the keyhole will temporarily constrict due to the melt pool dynamics whereby the keyhole pressure increases. By using a trailing flow orientation, the gas flow can directly interact with the keyhole rear wall. As a result, a dynamic pressure is applied to the rear wall, the keyhole is stabilized and kept open. When using a leading flow orientation, the gas flow is directed towards the keyhole front wall. Based on the inclination of the keyhole front, turbulences are initiated which result in a pressure loss. Following, the applied dynamic pressure is decreasing and the rear side of the keyhole cannot be stabilized sufficiently. Consequently, the keyhole is collapsing and spatter formation occurs.

#### 4. Summary

This paper describes the influence of local shielding gas flows on deep penetration laser welding of stainless steel (1.4301/ X5CrNi18-10/ AISI304) at high welding speeds of 8 m/min and above. In the first step, the influence of the angle of incidence as well as the flow rate was investigated in case of a trailing flow orientation. It could be shown, that the loss of mass could be reduced by up to 91 % by using the shielding gas flow at welding speeds of 10 – 16 m/min. Thereby, no noticeable difference could be determined by varying flow rates of 1.6 l/min to 6.4 l/min of argon. With increasing angles of incidence, it was possible to determine a reduction in the loss of mass, particularly at a welding speed of 12 m/min. By further investigations, the influence of the flow orientation could be examined. For this purpose, the trailing flow orientation was changed to a leading orientation. At a welding speed of 10 m/min, it was possible to achieve comparable results under both configurations. However, when welding at 12 m/min, the leading configuration resulted in a deterioration of the welding process. In conclusion, it can be stated that a trailing flow orientation is preferable to a leading flow orientation. Eventually, a description of the interaction between gas flow, keyhole fluctuations, pressure conditions and melt pool dynamics is given.

#### References

- Weberpals, J., 2010, Nutzen und Grenzen guter Fokussierbarkeit beim Laserschweißen, Dissertation Universität Stuttgart, in *Laser in der Materialbearbeitung*, Munich.
- Zhang, M., Cehn, G., Zhou, Y., Li, S., Deng, H., 2013, Observation of spatter formation mechanisms in high-power fiber laser welding of thick plate, in *Applied Surface Science* 280.
- Volpp, J., 2017, Keyhole stability during laser welding—Part II, in *Production Engineering* Bd. 11.
- Hügel, H., Graf, T., 2009, *Laser in der Fertigung*, Springer Verlag.
- Fabbro, R., Slimani, S., 2007, Melt pool dynamics during deep penetration CW Nd-Yag laser welding in *Proceedings of the Fourth Int. in WLT Conference on Lasers in Manufacturing*, Munich.
- Nagel, F., Brömme, L., Bergmann, J.P., 2019, Effects of two superimposed laser beams on spatter formation during laser welding of high alloyed steel, in *Journal of Laser Applications* 31 (2).
- Schmidt, L., Nagel, F., Friedmann, H., Reinhard, M., Bergmann, J.P., 2018, Potentiale angepasster Intensitätsverteilungen zur Spritzerreduzierung beim Laserstrahlschweißen, in *DVS-Berichte*, Bd. 346.
- Beck, M., 1996, Modellierung des Lasertiefschweißens, Universität Stuttgart, in *Laser in der Materialbearbeitung*.
- Kamikuki, K., Inoue, T., Yasuda, K., Muro, M., Nakabayashi, T., Matsunawa, A., 2002, Prevention of the welding defect by side gas flow and its monitoring method in continuous wave Nd:Yag laser welding, in *Journal of Laser Application*, Nr. 14.
- Fabbro, R., 2010, Melt pool and keyhole behaviour analysis for deep penetration laser welding, in *Journal of Physics D: Applied Physics*, Bd. 43.
- Herrmann, J., 2006, Prozessgase beim Laserschweißen Kostenfaktor oder Garant für wirtschaftliche, stabile und hochwertige Schweißverbindungen, in *DVS-Berichte* 241.
- Zhang, L., Zhang, J., Zhang, G., Bo, W., Gong, S., 2011, An investigation on the effects of side assisting gas flow and metallic vapour jet on the stability of keyhole and molten pool during laser full-penetration welding, in *Journal of Physics D: Applied Physics* 44.
- Schmidt, L., Hickethier, S., Schricker, K., Bergmann, J. P., 2019, Low-spatter high speed welding by use of local shielding gas flows, in *Proc. SPIE 10911, High-Power Laser Materials Processing: Applications, Diagnostics, and Systems VIII*, 109110V.